

Thermally induced capacitive effect of a nanoporous monel

Yu Qiao,^{a)} Venkata K. Punyamurtula, and Aijie Han
 Department of Structural Engineering, University of California—San Diego, La Jolla,
 California 92093-0085, USA

(Received 22 September 2006; accepted 23 September 2007; published online 8 October 2007)

As temperature changes, the equilibrium condition at a solid-liquid interface would be disrupted and the ion density varies, which, in turn, affects the interface potential. In the current study, this phenomenon is analyzed by using nanoporous monel electrodes. The experimental data show that, as the ion density is thermally adjusted, the capacitive effect leads to a significant thermal-to-electric energy conversion. © 2007 American Institute of Physics. [DOI: 10.1063/1.2798245]

At a solid-liquid interface, the motion of solvated ions in the interfacial double layer is thermally dependent.¹ Hence, if two interfaces of different temperatures form a circuit, due to the difference in interface capacities, there would be a net output voltage. However, in bulk materials, the associated electric energy is trivial.² Recent development of nanotechnology has provided a promising way to promote this capacitive effect. A dominant characteristic of a nanostructured material is its ultrahigh specific surface/interface area, usually millions of times larger than that of its bulk counterparts. For instance, the nanorod network at a gecko finger tip can greatly amplify the effect of van der Waals forces, making it much more adhesive.^{3,4} A nanoporous material, for another example, can be employed as a superabsorbent or a damper, as its large pore surface is exposed to functional liquids.⁵⁻⁷ It is envisioned that, if the thermally triggered interface ion redistribution can be achieved simultaneously across the large surface area of a nanostructured system, considerable electric energy can be generated.

In order to validate the above concept, we investigated a nanoporous monel containing connected nanopores.^{8,9} The pore size was around 480 nm. The material was provided by the Chand Eisenmann Metallurgical, Inc., in cylinder form, with the diameter of 9.5 mm and the height of 19.1 mm. The mass of each cylinder was 6.1 g. The thermoelectric system consisted of two identical nanoporous electrodes, as depicted in Fig. 1. Each electrode was formed by two monel cylinders. Prior to the test, they had been thermally treated in a tube furnace at 623 K for 12 h, with the desorbed gas being carried away by a nitrogen flow. The electrode was insulated from a copper counterelectrode by a 80 μm thick porous tissue. The insulation layer could actually be removed as long as the electrode and the counterelectrode did not contact each other. The electrodes were immersed in a 26 wt % aqueous solution of sodium chloride. The two counterelectrodes were connected directly by a copper wire, and the two nanoporous electrodes were connected through a 100 k Ω resistor, R_0 . The voltage over the resistor was measured by a National Instruments 6936E data acquisition board hosted by a Dell Latitude D600 computer. One of the electrode (“RT”) was maintained at room temperature (19 °C), and the other (“CT”) was heated by an Aldrich Z51 controlled-temperature coil. Initially, the temperatures of the two electrodes were the same, and the voltage across the resistor was zero. Then, the

temperature of electrode CT was increased at the rate of 0.5 °C/min. As shown in Fig. 2, a significant output voltage was generated, where ΔT was the temperature increase. When the temperature of CT reached 55 °C, it was maintained constant for a few minutes and the value of R_0 was changed in a broad range from 0.5 to 50 k Ω , and the output voltages ϕ are shown in Fig. 3. A comparison test was performed by replacing the nanoporous monel electrodes by solid monel rods of the same mass. When $R_0=1$ k Ω , no output electric energy could be detected.

As the temperatures of the two electrodes become increasingly different, ϕ rises monotonically. The output voltage increases from 0 to 112 mV as $\Delta T=36$ °C, indicating that thermal energy is converted to electric energy. If the electrode is a solid monel disk with a surface area of only a few cm^2/g , as the two electrodes are connected, the new equilibrium would be rapidly reached before the data acquisition system can detect any transient current. For a nanoporous electrode, the total surface area is 13.4 m^2 , and thus the thermoelectric energy conversion effect is largely amplified. According to Fig. 2, the ϕ - ΔT relationship is quite nonlinear. As the temperature difference is small, the temperature sensitivity of the output voltage α is relatively low, and it becomes increasingly large as ΔT rises. For instance, in the ΔT range of 30–36 °C, α is nearly constant at 8.7 mV/°C, a few times larger than that in the low ΔT stage. Compared with that of conventional thermoelectric materials such as complex oxides, superlattices, and nanowires/nanotubes,¹⁰ this value is order-of-magnitude higher.

Usually, thermoelectric energy conversion is achieved through the Seebeck effect. As the two ends of a conductor or a semiconductor are exposed to different temperatures, a net electron flow would be generated.¹¹⁻¹³ The energy conversion efficiency is often measured by the dimensionless figure of merit: $ZT=\alpha^2/\kappa\lambda$, where $\alpha=\phi/\Delta T$ is the Seebeck coefficient, κ is the electric resistivity, and λ is the thermal conductivity. In order to maximize energy conversion efficiency, the thermal conductivity must be minimized, so that thermal shorting can be minimized.¹⁴⁻¹⁷ The nanoporous monel system investigated in the current study is based on the capacitive effect and, thus, the ordinary definition of figure of merit cannot be applied. The nanoporous electrode can be regarded as an ion “reservoir.” At a constant temperature, a certain amount of ions would be absorbed at the nanopore surface. As temperature changes, ions are either absorbed or desorbed, depending on whether the interface capacity increases. Correspondingly, a net output voltage is generated.

^{a)} Author to whom correspondence should be addressed. Electronic mail: yqiao@ucsd.edu

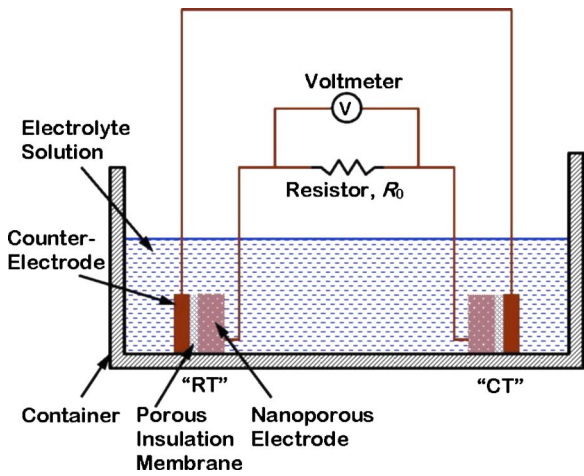


FIG. 1. (Color online) A schematic diagram of the experimental setup.

Although the two counterelectrodes, RT and CT, are connected by a copper wire, the thermal exchange between them is mainly through the liquid phase, since the mass of the copper wire is negligible compared with that of the electrolyte solution. This was validated by the experimental observation that if the copper wire was removed and the two counterelectrodes were grounded separately, there was little variation in system performance. In fact, if RT and CT are placed in two separate containers containing the same electrolyte solution, with the same temperature difference, the output voltage would be similar to that shown in Fig. 2. Under this condition, the two electrodes are isolated and the thermal exchange between them is negligible. Thus, the energy conversion efficiency should be close to the limit of Carnot cycle.

With a constant temperature difference of $\Delta T = 36^\circ\text{C}$, as the external resistance R_0 is decreased, as shown in Fig. 3, the output voltage is lowered. Eventually, when R_0 is reduced to zero, the circuit is shorted and ϕ vanishes. The nanoporous electrode can be regarded as a current source I_0 . The internal resistance of the electrolyte solution R_p is parallel to I_0 . The output voltage over R_0 is

$$\phi = I_0 R_p R_0 / (R_p + R_0). \tag{1}$$

As I_0 is taken as $32.6 \mu\text{A}$ and R_p is taken as $2 \text{ k}\Omega$, the difference between the theoretical results and the experimen-

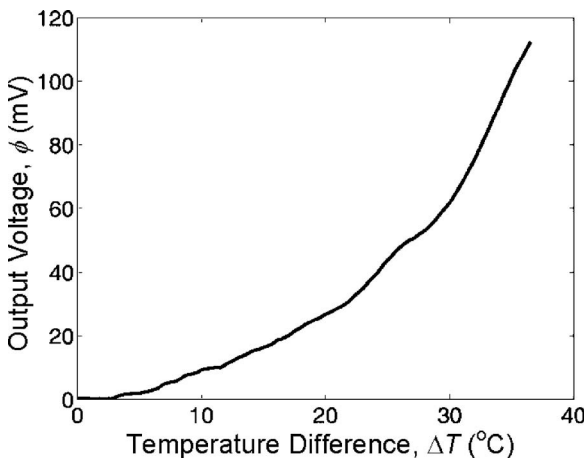


FIG. 2. The output voltage as a function of the temperature difference.

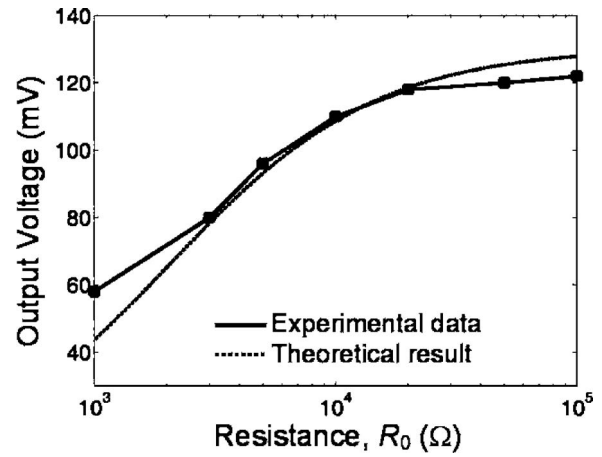


FIG. 3. The output voltage as a function of the external resistance R_0 . The temperature difference is 36°C .

tal data is minimized. Note that the system impedance is a function of the temperature, the temperature difference, as well as the total surface area, which cannot be captured by Eq. (1).

The potential difference across the electrode-liquid interface in the current study is smaller than 0.2 V , insufficient to activate any electrochemical reactions. As temperature changes, since the equilibrium condition in the outer Helmholtz plane cannot be reached, the output voltage would keep increasing. If the temperature difference of the two electrodes is constant, initially as the charges move from the high-potential electrode to the low-potential one, the nanoporous monel behaves as a “capacitor” that is both ion and electron conductive. As the new equilibrium is approached, the output voltage would decrease to zero (see Fig. 4). The decay of ϕ was quite slow. In the first 2 h, ϕ dropped by only 8%, and it took more than 5 days for the voltage to decrease by 80%. Once the two electrodes were disconnected and internally grounded, the initial equilibrium condition could be restored in a few minutes. Then, as they were connected again, the output voltage was recovered and the energy conversion process could be repeated, as shown by section “CD” in Fig. 4.

To summarize, it is validated that thermal effect on solid-liquid interface capacity can be significantly amplified by using nanoporous monel electrodes. With a relatively small

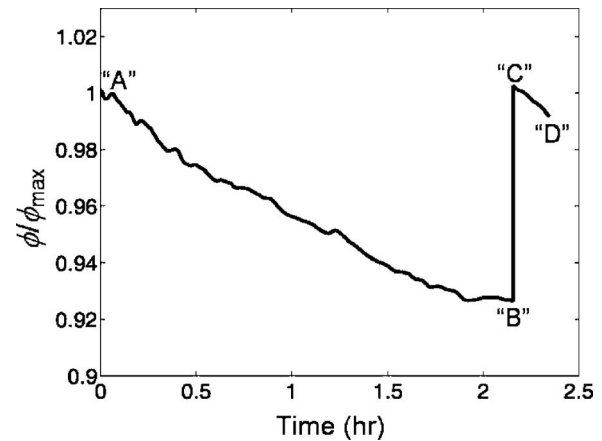


FIG. 4. The output voltage as a function of time as ΔT is kept at 36°C , where ϕ_{max} is the initial output voltage. The external resistance is $10 \text{ k}\Omega$.

temperature change of 36 °C, the output voltage is higher than 0.1 V. The thermal-to-electric energy conversion mechanism is related to the thermally aided diffusion of ions at pore surfaces, rather than the Seebeck effect. If the temperature difference is constant, the output voltage would vanish. However, the energy conversion capacity can be recovered as the electrodes are disconnected and internally grounded.

This study was supported by the Army Research Office under Grant No. W911NF-05-1-0288.

¹V. S. Bagotsky, *Fundamentals of Electrochemistry* (Wiley, New York, 2005).

²I. Williams, *Environmental Chemistry: A Modular Approach* (Wiley, New York, 2001).

³M. Sitti and R. S. Fearing, *J. Adhes. Sci. Technol.* **17**, 1055 (2003).

⁴B. X. Wang and X. P. Zhao, *Adv. Funct. Mater.* **15**, 1815 (2005).

⁵A. Han and Y. Qiao, *J. Am. Chem. Soc.* **128**, 10348 (2006).

⁶A. Han, X. Kong, and Y. Qiao, *J. Appl. Phys.* **100**, 014308 (2006).

⁷F. B. Surani and Y. Qiao, *J. Mater. Res.* **21**, 1327 (2006).

⁸V. I. Lozinsky, F. M. Plieva, I. Y. Galaev, and B. Mattiasson, *Bioseparation* **10**, 163 (2001).

⁹S. Polarz and B. Smarsly, *J. Nanosci. Nanotechnol.* **2**, 581 (2002).

¹⁰R. S. Figliola and D. E. Beasley, *Theory and Design for Mechanical Measurement* (Wiley, New York, 2000).

¹¹R. Decher, *Energy Conversion: Systems, Flow Physics, and Engineering* (Oxford University Press, London, 1994).

¹²S. Sieniutycz and A. De Vos, *Thermodynamics of Energy Conversion and Transport* (Springer, New York, 2000).

¹³T. M. Tritt and M. A. Subramanian, *MRS Bull.* **31**, 188 (2006).

¹⁴K. Koumoto, I. Terasaki, and R. Funahashi, *MRS Bull.* **31**, 206 (2006).

¹⁵H. Bottner, G. Chen, and R. Venkatasubramanian, *MRS Bull.* **31**, 211 (2006).

¹⁶A. M. Rao and T. M. Tritt, *MRS Bull.* **31**, 218 (2006).

¹⁷J. Yang and T. Caillat, *MRS Bull.* **31**, 224 (2006).